20210901_JI_Hydrodynamic_analisis_at_ht_Confluence__3918.pdf

by

Submission date: 09-Dec-2021 01:23PM (UTC+0700)
Submission ID: 1725269212
File name: 20210901_JI_Hydrodynamic_analisis_at_ht_Confluence__3918.pdf (1.22M)
Word count: 5394
Character count: 25193

Design Engineering

ISSN: 0011-9342 | Year 2021
Issue: 6 | Pages: 5186-5202

Hydrodynamic Analysis at The Confluence of The Mahakam River and The Karang Mumus Tributary

A. Nur [1], D. A. Suriamihardja[2], M. A. Thaha[3] and M. P. Hatta[4]

[1]Doctoral Course Student, Civil Engineering Department, Hasanuddin University
[2]Professor, Geophysics Department, Hasanuddin University
[3]Professor, Civil Engineering Department, Hasanuddin University
[4]Associate Professor, Civil Engineering Department, Hasanuddin University
[1]alpiansipilunhas@gmail.com*, [2]dahmaduh@gmail.com, [3]athaha_99@yahoo.com,
[4]mukhsan.hatta@unhas.ac.id

Abstract:

This study aimed to model the distribution pattern of water masses by considering the upstream discharge and the tidal elevation downstream. The method of this study carried out field observations as inputs required in numerical simulations. The field observations covered upstream discharge of Mahakam River and two-position of tidal levels, a river mouth of Mahakam River, and the river mouth of Karang Mumus. Upstream discharge is obtained about 83.74 m^3/s by measuring the current velocity and cross-section of the river on July 25, 2018. The tidal measurements have conducted for 15 days from July 14 to 28, 2018 (1-15 Dzulqa'dah 1439) in two-position of observations, namely Muara Pegah and the lower reaches of the Karang Mumus River. The former position has a tidal range of 192.42 cm, and the latter is 114.32 cm. There were 12 positions along the Mahakam River to measure salinity covered the results in the range of 28 to 0.05 PSU (practical salinity unit). Along the Karang Mumus River, 22 positions to measure salinity covered in 0.14 to 0.03 PSU. The currents and salinities in the Mahakam River have been distributed as maps by numerical simulations using mike21 software. Comparison between observed maps and numerical simulations give a good agreement by validation error of 6.14 % in Mahakam River mouth (Muara Pegah), and lower reaches of the Karang Mumus River of 3.41% and 6.6%. The seawater turned brackish, detected 14 km from the open sea at a high tide during the spring tide. Horizontal spatial distribution of salinity for SE-1 ranges 28 to 18 PSU as far as 5.2 km, SE-2 12 to 18 PSU as far as 7 km, SE-3 10 to 12 PSU as far as 9 km, and SE-4 4 to 10 PSU as far as 14 km from the open sea. Further far from the open sea, SE-5 was nearly freshwater. Well-mixed in the SE-3 area was caught 6.5 to 9.8 km from the open sea during spring and neap tides. High salinity causes the suspended load to flocculate until it falls into bedload. So, it is known the appearance of bars from the spatial distribution of horizontal salinity. On the other hand, the salinity intrusion persisted at the confluence of the Mahakam River and the Karang Mumus tributary, which is 60 km from the open sea. The minimum value was in the range of 0.065 to 0.240 PSU, but the minimum salinity

ISSN: 0011-9342 | Year 2021
Issue: 6 | Pages: 5186-5202

value is essential in research for early warning of future floods because freshwater affects salinity.

Keywords: Tidal levels, Currents, Salinities, and Numerical Modelling.

I. INTRODUCTION

In general, each river flow has different characteristics and forms from one another, not to mention the confluence of the Mahakam River and Karang Mumus Tributary. Several published studies on the Karang Mumus River are available, such as flow characteristics [8], preliminary mixing [10], deposition [9], analytical approach of long waves dynamics in an estuary [12]. Several previous studies use hydrodynamic modeling concerning rives and estuaries dynamics. Among them, the topics are relating to velocity distribution modeling [1], tidal effects [3], salinity and temperature [4][5], and sediment texture and topography feature control on the coastal morphodynamic state.

The current pattern of one of the generators is the tidal wave. Tidal dynamics gives three main consequences [6]: increasing mixing, partially suppressed the buoyancy effect, the river-ocean interface moves in vertical and horizontal directions, and two-way sediment transport is present. When the tide enters the river, it behaves like a wave that goes upstream, distorts, and eventually disappears due to the friction of the bottom and the river's flow. The tides from the sea enter the Mahakam River as far as 140 km [7]. At the same time, the area of Samarinda City is 60 km from the sea. Tidal water from the sea carries water mass, one of which is salinity. How far the salt wedge can have and where the perfect mixing occurs will be a good reason for developing research. This study aimed to model the distribution pattern of water mass with a 2D numerical model in the Mahakam River and Karang Mumus Tributary confluence based on the hydrodynamic effect of a discharge from upstream and tides from downstream.

II. MATERIALS AND METHODOLOGY

2.1. Research locations

Figure 1.A showed the research location at the confluence of the Mahakam River and the Karang Mumus tributary with its depth contours. Geographically, the confluence of the Mahakam River and the Karang Mumus tributary is located at 0°19'28.93" South Latitude - 0°26'54.72" South Latitude and 117°12'06.24" East Longitude - 117°15' 41.27" East Longitude. Administratively, the Karang Mumus river is in the area of Samarinda City and Kutai Kartanegara Regency. The confluence of the Mahakam River and the Karang Mumus tributary had a contour depth of -5 m to -48 m, while the depth from upstream to downstream of the Karang Mumus River ranged from -1 m to -5 m. Figure 1.B showed the location of the Mahakam River to Muara Pegah along 60 km. Muara Pegah in the Mahakam Delta has a contour depth of between -1 m to -5 m.

Design Engineering
ISSN: 0011-9342 | Year 2021
Issue: 6 | Pages: 5186-5202

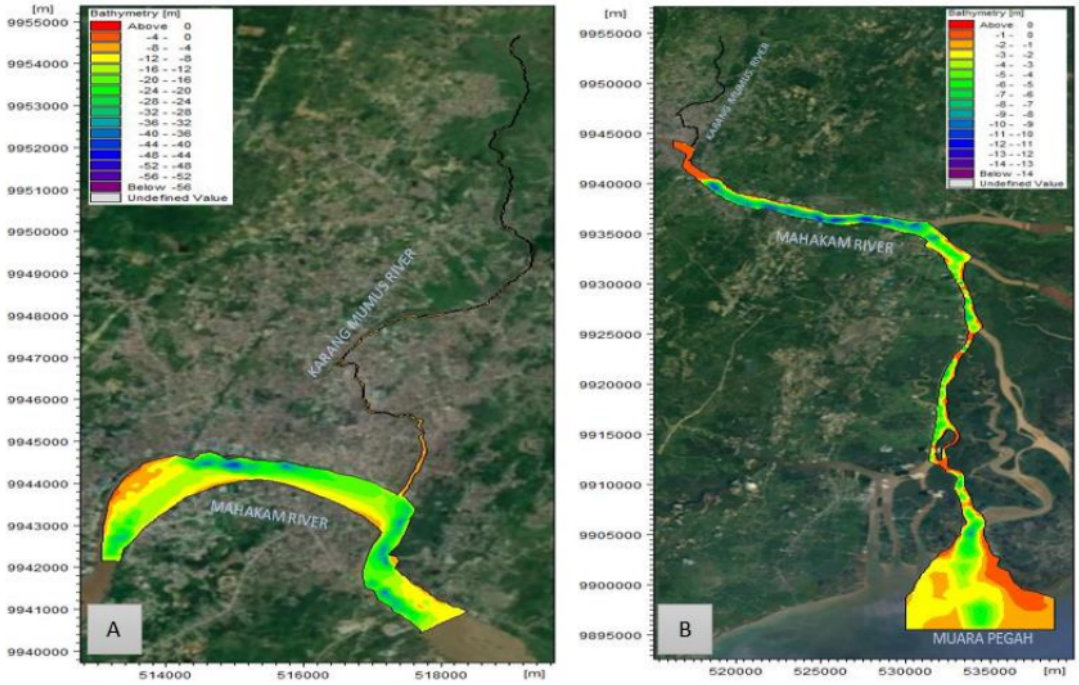

Fig 1. A. Location of the confluence of the Mahakam River and the Karang Mumus River; B. Mahakam River to Muara Pegah from the Mahakam Delta with depth contours.

2.2. Data

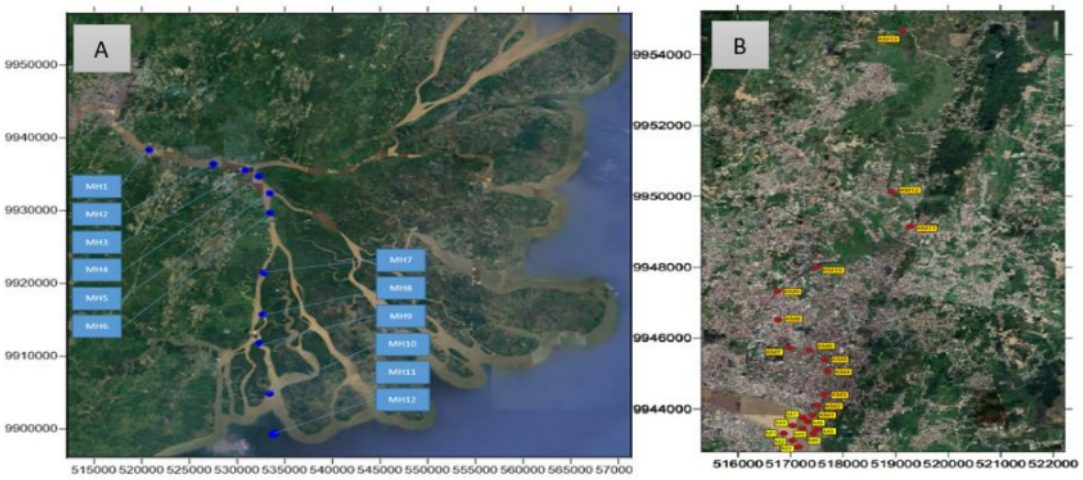

Fig 2. A. CTD point from Muara Pegah to Mahakam River; B. CTD point from Mahakam River to upstream of Karang Mumus River

ISSN: 0011-9342 | Year 2021
Issue: 6 | Pages: 5186-5202

The results of field measurements using CTD can be seen in Figure 3.A, which shows the Salinity Intrusion of Muara Pegah to the Mahakam River from point MH12 with a salinity of 28 PSU pushing into MH7 with a salinity of 5 PSU as far as 20 km, then holding fresh water at point MH6 to point MH1 which ranges from 0.05 - 2.5 PSU. The salinity value continued to decline until it reached the confluence of the Mahakam River and the Karang Mumus tributary M1 - M9 see picture 3.B. There was still salinity intrusion in the upstream part of M3, the middle part of the lower Mahakam River (M6) and the outflow location of the Karang Mumus River (M7 and M9) ranging from 0.1 to 0.03 PSU. Then moved to the Karang Mumus River in Figure 3.C. The salinity intrusion is cocked in the middle from upstream to downstream, ranging from 0.115 to 0.14 PSU vertically.

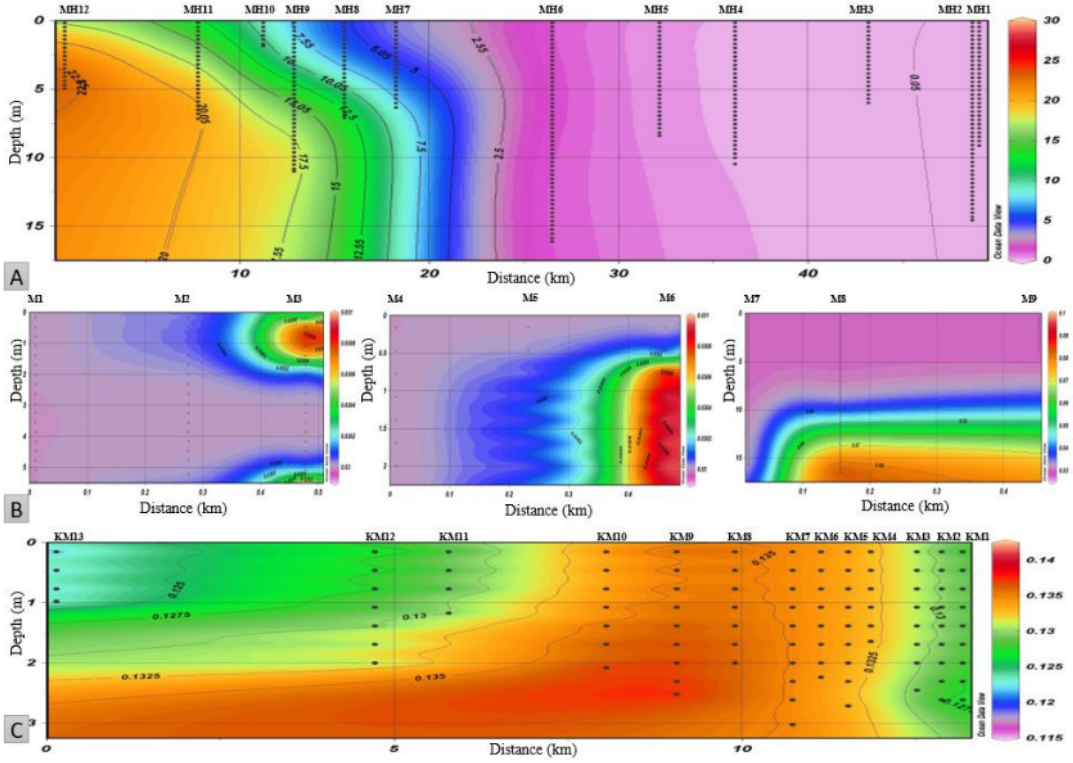

Fig 3. A. The salinity of Muara Pegah to the Mahakam River (MH12 - MH7) from 28 PSU to 5 PSU as far as 20 km, then (MH6 - MH1) was fresh water in the range of 0.05 - 2.5 PSU; B. Salinity at the confluence of the Mahakam River and the Karang Mumus River with intrusion in the upstream part of the M3, the lower Mahakam River (M6), and the outflow section of the Karang Mumus River (M7 and M9) ranged from 0.1 to 0.03 PSU; C. The salinity of the Karang Mumus River was in the middle from upstream to downstream, ranging from 0.115 to 0.14 PSU vertically.

The tidal measurements have conducted for 15 days from July 14 to 28, 2018 (1-15 Dzulqa'dah

ISSN: 0011-9342 | Year 2021
Issue: 6 | Pages: 5186-5202

1439) in two-position of observations. The first is at Muara Pegah, and the second is at the lower reaches of the river of Karang Mumus shown in Figure-4. The former position has a tidal range of 192.42 cm, and the latter is 114.32 cm. Upstream discharge is obtained about 83.74 m3/s by measuring the current velocity and cross-section of the river on July 25, 2018 at Muara Kaman District where is no longer affected by sea tides. Measurement of the discharge of the Karang Mumus River since on 14 - 28 July 2018 with average river discharge of 1.8 m3/sec measured in front of the flow exit of the Benangga Weir.

The current velocity of Muara Pegah was measured on July 25, 2018 with two points, namely: P1 at 9:00 = 0.48 m/s, P1 at 10:00 = 0.51 m/s, P1 at 11:00 = 0.49 m/s P2 at 15:00 = 0.09 m/s, P2 at 16:00 = 0.02 m/s and P2 at 17:00 = 0.14 m/s. Meanwhile, the velocity of the confluence of the Mahakam River and the Karang Mumus tributary was measured on July 25 2018 with three points ranging from 0.02 to 0.07 m/s.

2.3. Tidal Potential

In general, the tides are divided into four types [11]:

$$F = \frac{A_{K_1} + A_{O_1}}{A_{M_2} + A_{S_2}} \quad \text{.....(1)}$$

where K_1, O_1, M_2 and S_2 the main tidal components are diurnal (indeks 1) and semi-diurnal (indeks 2). Formzhal numbers are classified as $0 < F < 0.25$ — semidiurnal; $0.25 < F < 1.5$ — Mixed, predominantly semi-diurnal tide; $1.5 < F < 3.0$ — Mixed, predominantly diurnal tide; $F > 3.0$— Mixed, predominantly diurnal tide.

2.4. Hydrodynamic Model

The 2D flexible mesh numerical model is a numerical solution model based on a flexible mesh with ease of completion and advantages in configuring shorelines and bathymetry. This numerical calculation can be applied to the study of oceanographic, coastal, and estuary environments. Numerical solution of the two-dimensional incompressible Reynolds averaged Navier-Stokes equations using Boussinesq assumptions and hydrostatic pressure. The model consists of equations of continuity, momentum, temperature, salinity and density, and turbulent closure scheme. Numerical method using finite volume. The following equation is for the 2D solution [2]. The continuity equation is given:

$$\frac{\partial h}{\partial t} + \frac{\partial h\bar{u}}{\partial x} + \frac{\partial h\bar{v}}{\partial y} = S \quad \text{.....(2)}$$

The two horizontal equations of momentum for the x and y-component are:

Design Engineering

ISSN: 0011-9342 | Year 2021
Issue: 6 | Pages: 5186-5202

$$\frac{\partial h\bar{u}}{\partial t}+\frac{\partial h\bar{u}^2}{\partial x}+\frac{\partial h\overline{vu}}{\partial y}$$
$$=-gh\frac{\partial \eta}{\partial x}-\frac{h}{\rho_0}\frac{\partial p_a}{\partial x}-\frac{gh^2}{2\rho_0}\frac{\partial \rho}{\partial x}+\frac{\tau_{sx}}{\rho_0}-\frac{\tau_{bx}}{\rho_0}-\frac{1}{\rho_0}\left(\frac{\partial s_{xx}}{\partial x}+\frac{\partial s_{xy}}{\partial y}\right)$$
$$+\frac{\partial}{\partial x}(hT_{xx})+\frac{\partial}{\partial y}(hT_{xy})+hu_sS \qquad \text{.....(3)}$$

$$\frac{\partial h\bar{v}}{\partial t}+\frac{\partial h\overline{uv}}{\partial x}+\frac{\partial hv^2}{\partial y}$$
$$=-gh\frac{\partial \eta}{\partial y}-\frac{h}{\rho_0}\frac{\partial p_a}{\partial y}-\frac{gh^2}{2\rho_0}\frac{\partial \rho}{\partial y}+\frac{\tau_{sy}}{\rho_0}-\frac{\tau_{by}}{\rho_0} \qquad \text{.....(4)}$$
$$-\frac{1}{\rho_0}\left(\frac{\partial s_{yx}}{\partial x}+\frac{\partial s_{yy}}{\partial y}\right)+\frac{\partial}{\partial x}(hT_{xy})+\frac{\partial}{\partial y}(hT_{yy})+hv_sS$$

where the settlement indicates the value of the average depth, and $\bar{u}$ and $\bar{v}$ are the depth-averaged velocities, given by:

$$h\bar{u}=\int_{-d}^{\eta}udz,\qquad h\bar{v}=\int_{-d}^{\eta}vdz \qquad \text{.....(5)}$$

where t is the time; x and y are the Cartesian coordinates; η is the surface elevation; d is the still water depth; $h=\eta+d$ is the total water depth; g is the gravitational acceleration; ρ is the density of water; ρ_0 is the reference density of water; s_{xx}, s_{xy}, s_{yx} dan s_{yy} is components of the radiation stress tensor; S is the magnitude of the discharge; τ_{sx}, τ_{sy} and τ_{bx}, τ_{by} are the x and y components of the surface wind and bottom stresses; u_s , v_s is the velocity by which the water is discharged into the ambient water. The lateral stresses T_{ij} include viscous friction, turbulent friction and differential advection. The eddy viscosity formulation based on of the depth average velocity gradients.

$$T_{xx}=2A\frac{\partial \bar{u}}{\partial x},\qquad T_{xy}=A\left(\frac{\partial \bar{u}}{\partial y}+\frac{\partial \bar{v}}{\partial x}\right),\qquad T_{yy}=2A\frac{\partial \bar{v}}{\partial y} \qquad \text{.....(6)}$$

where T_{xx}, T_{xy} dan T_{yy} adalah viscous friction, A adalah the horizontal eddy viscosity.

The transport equation for salt and temperature is obtained by the following two-dimensional transport equation.

$$\frac{\partial h\bar{T}}{\partial t}+\frac{\partial h\bar{u}\bar{T}}{\partial x}+\frac{\partial h\bar{v}\bar{T}}{\partial y}=hF_T+h\hat{H}+hT_sS \qquad \text{.....(7)}$$

$$\frac{\partial h\bar{s}}{\partial t}+\frac{\partial h\bar{u}\bar{s}}{\partial x}+\frac{\partial h\bar{v}\bar{s}}{\partial y}=hF_s+hs_sS \qquad \text{.....(8)}$$

ISSN: 0011-9342 | Year 2021
Issue: 6 | Pages: 5186-5202

where $\overline{T}$ and $\bar{s}$ is the depth average temperature and salinity; $\hat{H}$ is a source term due to heat exchange with the atmosphere; F_T and F_s are the horizontal diffusion Temperature and Salinity terms. T_s and s_s are source temperature and salinity

2.5. Model Calibration

The model calibration was chosen as the error statistic using RMSE [14]. RMSE is calculated based on the equation:

$$RMSE = \sqrt{\frac{\sum_{t=1}^{n}(A_t - F_t)^2}{n}} \quad \text{.....(9)}$$

where A_t is actual data value; F_t is forecast value; n is number of data

2.6. Boundary Condition

The current and salinity modeling design included tidal time series data, bathymetric mesh data, and salinity data. The boundary conditions made, namely: BC 1 using land, BC 2 using tidal observation data, BC 3 using the Mahakam River current velocity value as an observation, and BC 4 using the current velocity value of the Karang Mumus river as an observation. modeling was carried out on four conditions, namely high tide during spring tide, low tide during spring tide, high tide during the neap tide, low tide during neap tide

III. RESULTS AND DISCUSSION

3.1. Boundary Condition

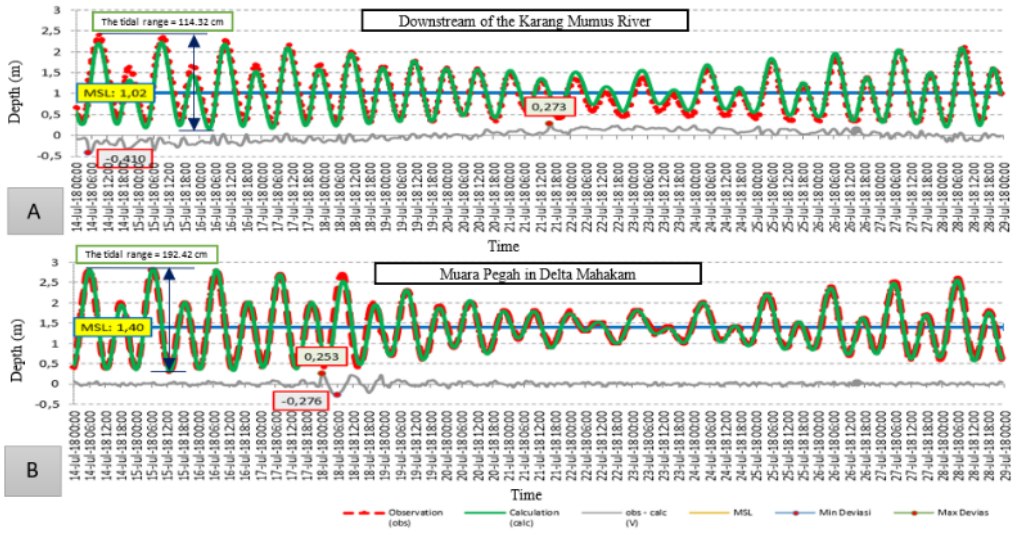

Fig 4. A. Tidal Chart at downstream of the Karang Mumus River with a tidal range of 114.32

ISSN: 0011-9342 | Year 2021
Issue: 6 | Pages: 5186-5202

cm; B. Tidal Chart at Muara Pegah in the Mahakam Delta with a tidal range of 192.42 cm for 15 days used the LeastSquare method

Figure 4.A showed that the Tidal Graph in the lower reaches of the Karang Mumus River with a tidal range of 114.32 cm, and Figure 4.B shows the Tidal Graph at Muara Pegah in the Mahakam Delta with a tidal range of 192.42 cm during 15 days using the LeastSquare method. The difference in tidal range was 78.1 cm at the two observation points. The tidal range at Muara Pegah was higher than the tidal range at the lower reaches of the Karang Mumus River. Tidal Validation for the lower reaches of the Karang Mumus and Muara Pegah rivers obtained standard deviations = 0.132 and 0.057, and results show that the Formzhal numbers show mixed, predominantly semi-diurnal tides.

3.2. Flow Pattern

1. Flow pattern in Muara Pegah

When the high tide of the spring tide showed an inflow from the sea to the mouth of the estuary area with current speeds ranging from 0.05 – 0.15 m/s from the southeast, the south direction went from 0.15 – 0.55 m/s while the west Power ranges from 0.15 – 0.75 m/s. The Southwest Direction had a more dominant speed when entering the estuary. The rate increased when there was a narrowing of the river body and decreased when the river widened. The current pattern at low tide during the spring tide in Muara Pegah. The outflow from the upstream with speed ranging from 0.025 – 0.075 m/s then the current velocity in the estuary ranged from 0.05 – 0.35 m/s spreading towards the Southeast, South and dominantly towards the Southwest. Variations in current speed were caused, namely: differences in morphology and slope of the bottom.

The current pattern at high tide during the neap tide, the current speed was evenly distributed along with the upstream to downstream of Muara Pegah around 0.04 – 0.16 m/s, but when the water entered the bifurcation, the current rate changed to move fast with a range of 0.28 – 0,56 m/s. Meanwhile, the current pattern of the water receded during the neap tide. The current accelerated two times. First, When the water came out of the bifurcation into a river, the increase in current velocity was about 0.25 – 0.52 m/s. Second, when it met a shallow area before reaching the estuary's mouth with current speeds ranging from 0.05 – 0.12 m/s. The flow pattern of these two conditions was still in the same direction, namely Southwest, South, and Southeast.

Design Engineering
ISSN: 0011-9342 | Year 2021
Issue: 6 | Pages: 5186-5202

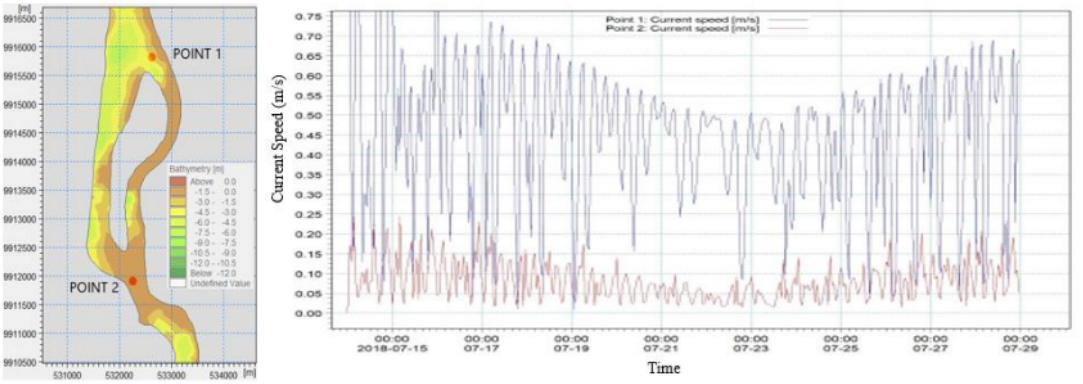

Fig 5. Field current measurement points with depth contours along with graphs of simulation of current velocity for 15 days at points 1 and 2 in Muara Pegah

Current speed made real-time for 15 days. The rate of moving during that period by determining the point adjusted to the field measurements. Figure 5 showed the same point as the field measurements to validate the average current velocity direction. The upstream speed was faster than the downstream, as seen from Figure 5.

2. Flow Patterns at the confluence of the Mahakam River and Karang Mumus Tributary

The current speed downstream of the Mahakam River ranged from 0.1 to 0.2 m/s in high tide when the spring tide at the confluence of the Mahakam River and the Karang Mumus River. The current increase in the narrowing cross-section of the river before heading towards the confluence of the Mahakam River and the Karang Mumus Tributary and when the tide entered the Karang Mumus River at speeds ranging from 0.12 – 0.22 m/s. This is because the cross-section of the Karang Mumus River is smaller than the cross-section of the Mahakam River. At the upper reaches of the Mahakam River, there was a decrease in current speed ranging from 0.02 to 0.16 m/s. The outflow from the upstream of the Mahakam River ranged from 0.1 to 0.165 m/s when the water receded at the spring tide at the confluence of the Mahakam River and the Karang Mumus Tributary. Then it slowed down until it met the outflow of the Karang Mumus River. The vortex occurred in the eastern area near the mouth of the confluence of the Mahakam River and the Karang Mumus Tributary. The downstream speed of the Mahakam River ranged from 0.015 – 0.09 m/s. At the same time, the current velocity in the lower reaches of the Karang Mumus River ranges from 0.06 to 0.15 m/s.

The current velocity in high tide when neap tide at the confluence of the Mahakam River and the Karang Mumus Tributary was in the range of 0.015 – 0.03 m/s. Like a giant whirlpool, due to the meeting of the currents of the tide from the downstream of the Mahakam River and the water flowing from the upstream to the downstream of the Mahakam River at the confluence of the rivers. On the other hand, the current speed at low tide during the neap tide at the Confluence of

ISSN: 0011-9342 | Year 2021
Issue: 6 | Pages: 5186-5202

the Rivers seemed small, ranging from 0.015 – 0.18 m/s.

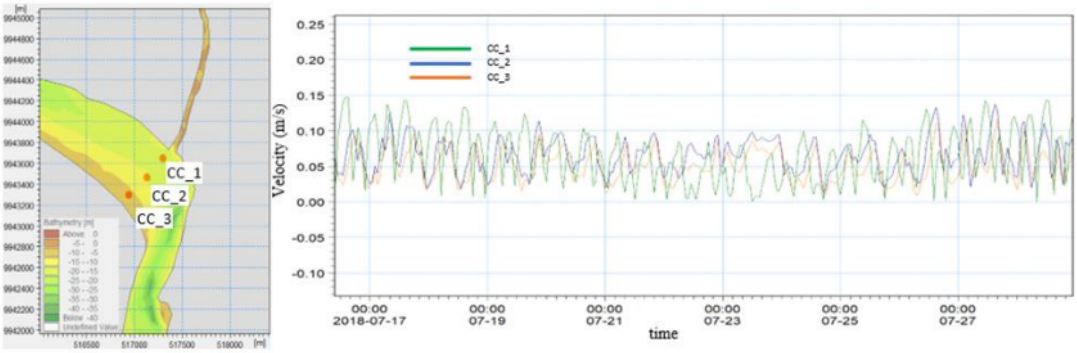

Fig 6. Field current measurement points with depth contours and simulation graphs of current velocity for 15 days at CC_1, CC_2, and CC_3 at the confluence of the Mahakam River and the Karang Mumus tributary.

Figure 6 shows 3 points Simulation current speed adjusted for field data retrieval. The current speed CC_1 was in the southwest direction of the confluence of the river, CC_2 was in the middle of the confluence river, and CC_3 was on the outflow of the Karang Mumus River. Results show that the speed on CC_3 is greater than the others seen on the simulation graph of the current for 15 days.

3.3. Salinity Pattern Modeling in Muara Pegah and The Confluence of The Mahakam River and Karang Mumus Tributary

The southeast direction became the dominant current on the spring tide in the Pegah estuary, causing the salinity to be trapped in the western tip of the estuary's mouth. This was seen in the high tide and low tide conditions of the spring tide at the mouth of Muara Pegah. When the high tide at springtide as shown in Figure 7.A, the spatial distribution of SE1 coming from the sea was about 28-18 PSU moving upstream as far as 5.2 km from the southeast, SE2 between 12-18 PSU went upstream to 7 km, SE3 ranged from 10-12 PSU through 9 km upstream, SE4 with a range of 4-10 PSU moved 14 km upstream. SE5 is freshwater from river discharge. The seawater to brackish water was 14 km into the Mahakam River with a 28-5 PSU salinity. The well-mixed occurred at SE3 in the 7 – 9 km area of the open sea. Figure 7.B shows the low tide of the spring tide. SE1 spatial distribution was up to 4.8 km from the open sea, SE2 was up to 7 km, SE3 was 9.8 km, SE4 was 13.8 km away. SE5 as freshwater to SE4. The seawater to brackish water was located as far as 13.8 km with a salinity of about 28-5 PSU. The well-mixed occurred at SE3 in the region 7 – 9.8 km from the open sea.

When neap tide, the current was very dominant from the south to the north at high tide or vice versa at low tide, as shown in Figures 7.C and 7.D. This causes salinity to get stuck in both

ISSN: 0011-9342 | Year 2021
Issue: 6 | Pages: 5186-5202

directions during the neap tide. The spatial distribution of high tide and low tide during the neap tide, such as SE1, SE2, SE3, SE 4, we're only at the mouth of the estuary. Furthermore, SE5 was around 9.8 - 10 km from the open sea. On the other hand, the well-mixed occurred in SE3 in the range of 6.5 – 7 km from the open ocean.

The seawater salinity in the range of 28-5 PSU had stopped in the estuary area. Still, the tidal currents continued to move until the confluence of the Mahakam River and Karang Mumus Tributary. The salinity values that flowed in each part of the confluence of the Mahakam River and Karang Mumus Tributary did not vary enough because the salinity in the Mahakam River and Karang Mumus river had salinity values < 2 PSU, which means that the salinity conditions in the area were freshwater. Figure 8. A shows the salinity of high tide at spring tide conditions in the Mahakam River and Karang Mumus Tributary confluence, ranging from 0.128 PSU to 0.24 PSU.

Meanwhile, Figure 8.B showed low tide at neap tide in the confluence of the Mahakam River and Karang Mumus Tributary of 0.138 PSU – 0.222 PSU. The spatial distribution of salinity when the low tide on the springtide from SC1, SC2, SC3, SC4, and SC5 move in following the tidal currents.

Design Engineering

ISSN: 0011-9342 | Year 2021
Issue: 6 | Pages: 5186-5202

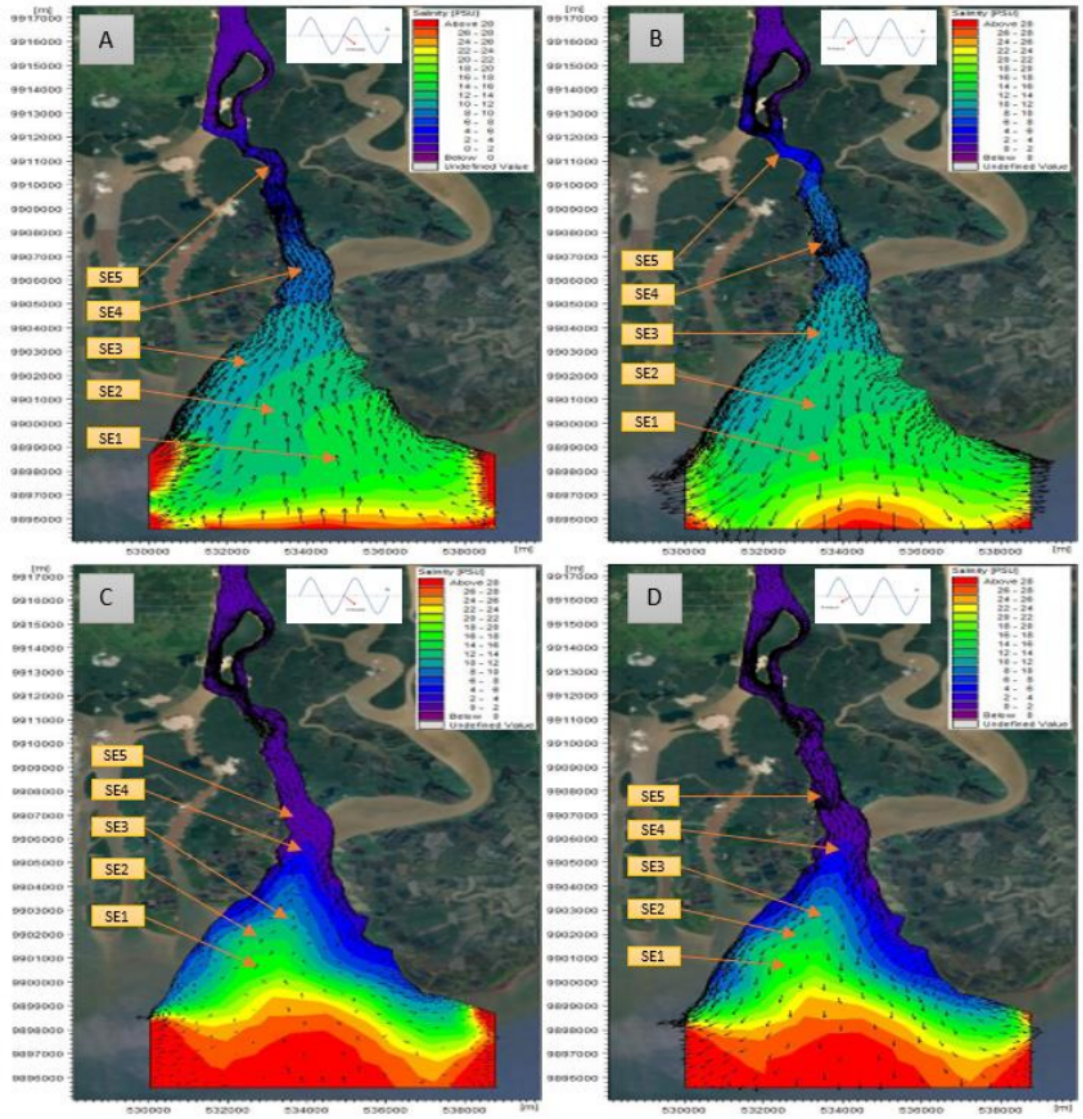

Fig 7.A. Spatial distribution of horizontal salinity with current velocity and direction at high tide during spring tide with SE1 (28 – 18 PSU) intrusion 5.2 km, SE2 (12 – 18 PSU) 7 km, SE3 (10 – 12 PSU) 9 km, SE4 (4 – 10 PSU) 14 km from the open sea; B. The SE1 intrusion was 4.8 km, SE2 7 km, SE3 9.8 km, SE4 13.8 km from the high seas at low tide during the spring tide; C. The SE1 intrusion was 5 km, SE2 6.8 km, SE3 7.2 km, SE4 10 km from the open sea at high tide at neap tide; D. the SE1 intrusion was 4.5 km, SE2 6 km, SE3 7 km, SE4 9.8 km from the high seas and SE5 as freshwater at low tide during the neap tide in Muara Pegah

Design Engineering

ISSN: 0011-9342 | Year 2021
Issue: 6 | Pages: 5186-5202

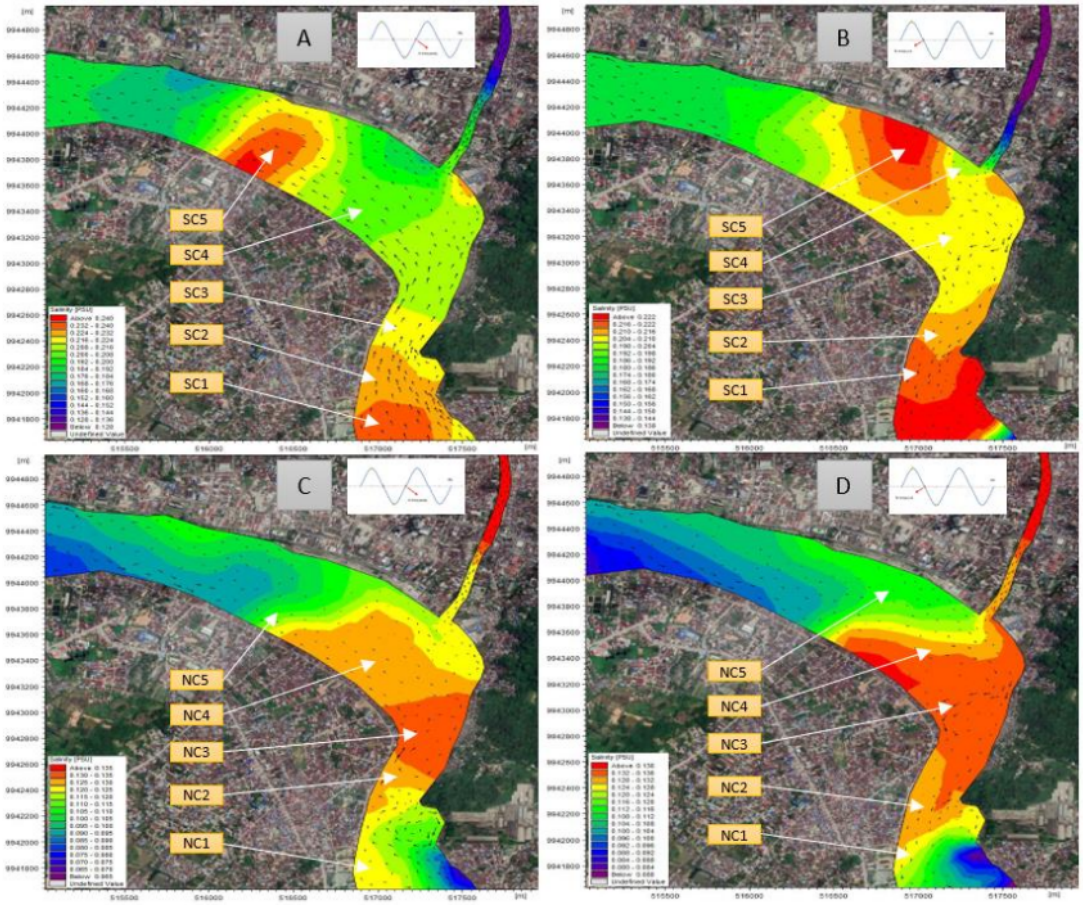

Fig 8.A. Spatial distribution of horizontal salinity along with the speed and direction of currents at high tide during spring tide. The salinity intrusion of SC1 (0.232 - 0.24 PSU) was 2 km, SC2 (0.224 - 0.232 PSU) 3 km, SC3 (0.216 - 0.224 PSU) 4.5 km, SC4 (0.2 - 0.208 PSU) 9 km from the downstream of the Mahakam River and SC5 (0.216 – 0.240) was deposited in the south; B. The SC1 intrusion was 3.2 km, SC2 5 km, SC3 5 - 12 km around the confluence of the river, SE4 was located in the outflow of the Karang Mumus River, and SC5 was deposited in the north in the water receding when the spring tide; C. The NC1 intrusion (0.12 - 0.125 PSU) was 3 km, NC2 (0.125 - 0.130 PSU) 4.5 km from the downstream, NC3 (0.130 - 0.135 PSU) was 6 km, NC4 (0.125 - 0.130 PSU) 9 km from the lower Mahakam River and NC5 (0.115 – 0.120) was 14 km spreading in the north at high tide when the neap tide; D. The NC1 intrusion was 2 km, NC2 4 km, NC3 2 - 6 km, NC4 seen 7 km from downstream Mahakam River and downstream of Karang Mumus River and NC5 was 14 km spreads in the north at low tide when the neap tide.

The high tide pattern also brought SC3 into the Karang Mumus river. Meanwhile, when the water receded on a neap tide, SC1, SC2, SC3, SC4, and SC5 headed downstream of the Mahakam River.

ISSN: 0011-9342 | Year 2021
Issue: 6 | Pages: 5186-5202

SC5 shifts from high tide to low tide due to the circular flow of the curved shape of the river. SC5, which was initially in the west at high tide, moved to the east. SC4 was only left downstream of the Karang Mumus River when the water receded due to a blockage from the Mahakam River's discharge which blocked the discharge from downstream Karang Mumus River.

The salinity of high tide at neap tide conditions in the confluence of the Mahakam River and Karang Mumus Tributary was 0,065 - 0,135 PSU as can be seen in Figure 8.C. While in Figure 8.D Salinity of the low tide at Neaptide in the confluence of the Mahakam River, and Karang Mumus Tributary was 0.08 - 0.136 PSU. The current velocity at neap tide seemed small. Therefore, the spatial distribution of salinity, such as NC1, NC2, NC3, NC4, and NC5, only swirled in the confluence of the Mahakam River and Karang Mumus Tributary. Overall both during Spring tide and Neap tide, the salinity value was small but still experienced changes due to the increase or decrease in fresh water at the meeting. The spatial distribution was also influenced by currents and the depth of the contours of these two rivers. This can be used as an early warning for flooding because the influence of freshwater will affect the value of salinity.

3.4. Validasi Arus

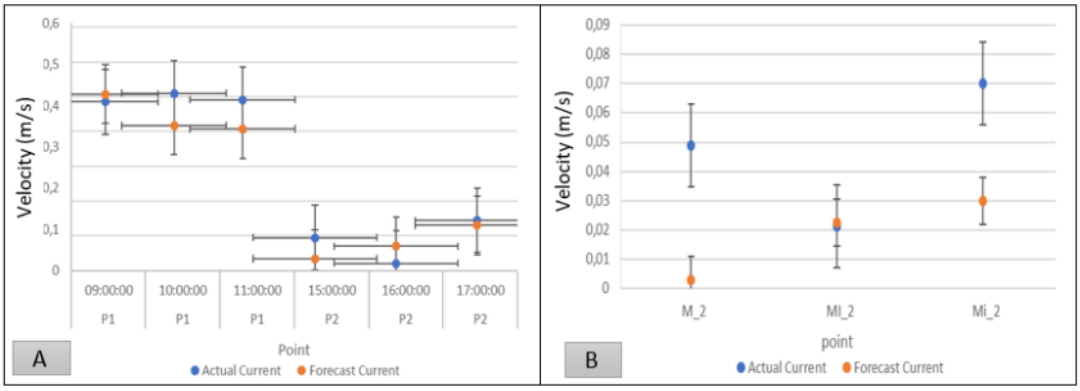

Fig 9. A. RMSE of current speed ū Muara Pegah in the Mahakam Delta; B. RMSE of current speed ū in the confluence of the Mahakam River and Karang Mumus Tributary

Based on the simulation graph of the current velocity in Muara Pegah and the confluence of the Mahakam River and Karang Mumus Tributary compared to field data on July 25, 2018. The results obtained RMSE of 6.14% and 3.41%, as shown in Figure 8. A and Figure 8.B.

Design Engineering
ISSN: 0011-9342 | Year 2021
Issue: 6 | Pages: 5186-5202

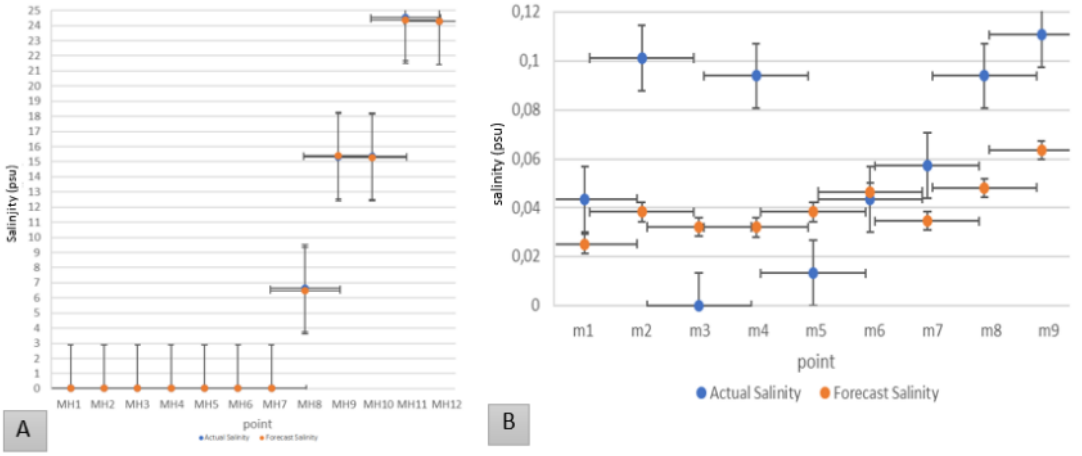

Fig 10. A. Validation of salinity data on modeling and measurement in Muara Pegah; B. Validation of salinity data on modeling and measurement in the confluence of the Mahakam River and Karang Mumus Tributary

Figure 9. A showed the validation of salinity data on modeling and measurement in Muara Pegah using 12 data. RMS Error results, salinity in Muara Pegah was 7.3%. While Figure 9.B showed the validation of salinity data on the Mahakam River and Karang Mumus Tributary confluence using 9 data. The results showed that the RMS Error salinity was 6.6%.

IV. CONCLUSION

During the spring tide, Results at Muara Pegah showed a horizontal spatial distribution of salinity for SE1, SE2, SE3, and SE4 as far as 5.2 km, 7 km, 9 km, 14 km from the open sea. SE5 was freshwater. Well mixed in, the SE3 area captured 6.5 – 9.8 km from the open ocean during spring and neap tides. Meanwhile, salinity intrusion still occurred at the confluence of the Mahakam River and the Karang Mumus tributary, which is 60 km from the open sea. Spatial distribution of horizontal salinity at spring tide. SC1, SC2, SC3, and SC4 salinity intrusions were seen 2 km, 3 km, 4.5 km, and 9 km downstream of the Mahakam River, and SC5 is between the confluence of the river and the upper Mahakam River and settles in the south during high tide and settles in the north at low tide.

In contrast, salinity intrusion on NC1, NC2, NC3, and NC4 basins were seen 3 km, 4.5 km, 6 km, and 9 km from the downstream of the Mahakam River and NC5 as far as 14 km spreading in the northern part. The current speed at neap tide seemed small so that the spatial distribution of salinity seemed to only swirl in the confluence area of the Mahakam River and the Karang Mumus tributary. Hydrodynamic modeling applied to the calculation of salinity will affect the velocity of the components that occur. In shallow water, the momentum function will work for the salinity equation. Changes in the force and salinity value are directly proportional to the effect of changes

ISSN: 0011-9342 | Year 2021
Issue: 6 | Pages: 5186-5202

in water level.

REFERENCES

1. Arafat Y, Pallu MS, Maricar F, and Lopa RT (2016). Hydrodynamics and Morphological Changes Numerical Model of the Jeneberang Estuary. IJIRAE, vol. 3, no. 8, pp. 21–29.
2. DHI Water and Environment (2012) a, MIKE21&MIKE3 Flow Model FM: Hydrodynamic and Transport Module Scientific Documentation, DHI, Agem Alle 5, DK-2970 Hersholm, Denmark.
3. Hatta MP, Thaha MA, Lakatua MP (2018). Simulation Model Pattern Distribution Sediment at Ambon Bay, Indonesia. MATEC Web of Conferences 203, 01009 published by EDP Sciences https://doi.org/10.1051/matecconf/201820301009
4. Karamma R (2018). Analysis of Coastal Sediment Transport in Estuary of Jeneberang and Tallo River Caused by Waves against Coast of Makassar. in ICMID
5. Karamma R, Pallu MS, Thaha MA, Hatta MP, Mustari AS, Sukri AS (2020). Analysis of Longshore Sediment Transport at Theestuaries of Jeneberang River and Tallo River Caused by Waves on Coast of Makassar. ICMID 2018, IOP Conf. Series: Materials Science and Engineering 797 012010, IOP Publishing
6. Leonardi N, Alexander S, Kolker AS, Fagherazzi S (2015), Interplay between river discharge and tides in a delta disTributary. Advances in Water Resources 80 69–78.
7. Mandang I, and Yanagi T (2008). Tide and tidal current in the Mahakam Estuary, East Kalimantan, Indoensia, Coastal Marine Science, (in press).
8. Nur A, Surimihardja DA, Thaha MA and Hatta MP (2019). Preliminary Modeling of Characteristics of Current and Batimetry in The Confluence of Mahakam River and Karang Mumus River. IJEScA, 6(1), pp 155-164.
9. Nur A, Surimihardja DA, Thaha MA and Hatta MP (2019). Preliminary sediment modeling at the confluence of the Mahakam and Karang Mumus River. ICCEE 2019. IOP Conf. Series: Earth and Environmental Science 419 012129. IOP Publishing.
10. Nur A, Surimihardja DA, Thaha MA and Hatta MP (2019). Type of mixing confluence between Mahakam and Karang Mumus Rivers based on temperature and salinity distribution tidally. ICCEE 2019, IOP Conf. Series: Earth and Environmental Science 419 012129. doi:10.1088/1755-1315/419/1/012139
11. Ongkosongo OSR and Suyarso (1989). Tidal. Research and Development Center for Oceanology LON LIPI, Jakarta. 257 pp.
12. Raming I, Suriamihardja DA, and Kusuma J (2019) Analytical Approach of Long Waves Dynamics in an Estuary (Case Study in Karang Mumus River Estuary). The 3rd International Conference On ScienceJournal of Physics: Conference Series 1341 (2019) 082036, IOP Publishing doi:10.1088/1742-6596/1341/8/082036
13. Suriamihardja DA, Thaha MA, Imran, AM (2015). Sediment Texture and Topography Features Control on Coastal Morphodynamics State. IJEScA.

ISSN: 0011-9342 | Year 2021
Issue: 6 | Pages: 5186-5202

14. Sutherland M, and Sylvester AK (2000), Advrtising and the Mind of the Consumer, ISBN 1741150140, 9781741150148

20210901_JI_Hydrodynamic_analisis_at_ht_Confluence__391...

ORIGINALITY REPORT

10%	7%	7%	4%
SIMILARITY INDEX	INTERNET SOURCES	PUBLICATIONS	STUDENT PAPERS

PRIMARY SOURCES

1	repositorio.unicamp.br Internet Source	1%
2	Submitted to Asian Institute of Technology Student Paper	1%
3	www.repository.cam.ac.uk Internet Source	1%
4	www.donpedro-relicensing.com Internet Source	1%
5	Jinlong Wang, Dekun Huang, Weiming Xie, Qing He, Jinzhou Du. "Particle Dynamics in a Managed Navigation Channel Under Different Tidal Conditions as Determined Using Multiple Radionuclide Tracers", Journal of Geophysical Research: Oceans, 2021 Publication	1%
6	journal.hep.com.cn Internet Source	1%
7	iahr.oss-cn-hongkong.aliyuncs.com Internet Source	1%

8	unmul.ac.id Internet Source	<1 %
9	seps.unsrat.ac.id Internet Source	<1 %
10	U Hernawan, F B Prasetio, R K Risdianto. "Numerical modeling of abrasion hazard in Senindara River, Bintuni Bay", IOP Conference Series: Earth and Environmental Science, 2020 Publication	<1 %
11	link.springer.com Internet Source	<1 %
12	Luiz Bruner de Miranda, Fernando Pinheiro Andutta, Björn Kjerfve, Belmiro Mendes de Castro Filho. "Fundamentals of Estuarine Physical Oceanography", Springer Science and Business Media LLC, 2017 Publication	<1 %
13	Nicoletta Leonardi, Alexander S. Kolker, Sergio Fagherazzi. "Interplay between river discharge and tides in a delta distributary", Advances in Water Resources, 2015 Publication	<1 %
14	Oke, P.R.. "The Bluelink ocean data assimilation system (BODAS)", Ocean Modelling, 2008 Publication	<1 %

15	B Bakri, A Sumakin, Y Widiasari, M Ihsan. "Distribution pattern of water salinity analysis in Jeneberang river estuary using ArcGIS", IOP Conference Series: Earth and Environmental Science, 2020 Publication	<1 %
16	www.grandeforetdanlier.be Internet Source	<1 %
17	www.hydrol-earth-syst-sci.net Internet Source	<1 %
18	Aizhen Liu, Ying Wang, Yuxin Zhu, Mingchang Li, Boqun Liu. "Hydrological observation and numerical simulation in Red Bay", IOP Conference Series: Earth and Environmental Science, 2018 Publication	<1 %
19	Gulustan Dogan, Rachel Carroll, Gozde Merve Demirci. "911 4 COVID-19: Analyzing Impact of COVID-19 on 911 Call Behavior", 2021 10th International Conference on Software and Computer Applications, 2021 Publication	<1 %
20	Majid Eskafi, Ragnar Ásmundsson, Steingrímur Jónsson. "Feasibility of seawater heat extraction from sub-Arctic coastal water; a case study of Onundarfjordur, northwest Iceland", Renewable Energy, 2019 Publication	<1 %

21	R Karamma, M S Pallu, M A Thaha, M P Hatta, M Ihsan. "Spatial mapping of water mass structure in the estuary of Jeneberang river", IOP Conference Series: Earth and Environmental Science, 2021 Publication	<1 %
22	R Karamma, M S Pallu, M A Thaha, M P Hatta. "Observation pattern of water mass structure at Jeneberang river estuary", IOP Conference Series: Earth and Environmental Science, 2020 Publication	<1 %
23	Xiu-juan Jiang, Yan Han, Jun Du, Ru-cheng Jiang. "Application of two-dimensional mathematical model in backwater calculation for flood control evaluation of mountainous rivers", IOP Conference Series: Earth and Environmental Science, 2019 Publication	<1 %
24	repository.tudelft.nl Internet Source	<1 %
25	sam.ucsd.edu Internet Source	<1 %
26	www.leonardo-hotels.com.pt Internet Source	<1 %
27	www.mdpi.com Internet Source	<1 %

28 "Ecology, Conservation, and Restoration of Chilika Lagoon, India", Springer Science and Business Media LLC, 2020 <1%

Publication

Exclude quotes	On	Exclude matches	< 5 words
Exclude bibliography	On		